Ind. J. Pharm. Edu. Res., 2027; 1-11.
https://www.ijper.org

Original Article

Diindolylmethane-Mediated Apoptosis and Cell Cycle Alterations in SK-BR-3 Breast Cancer Cells: Cellular, Molecular and In Silico Approaches

Rashed M. Almuqbil*

Department of Pharmaceutical Sciences, College of Clinical Pharmacy, King Faisal University, Al-Ahsa, SAUDI ARABIA.

ABSTRACT

Background: 3,3′-Diindolylmethane (DIM), a cruciferous-derived bioactive compound, has shown anticancer effects in various cancer models. However, the molecular mechanisms underlying its effects in breast cancer cells are still not fully understood. This study investigated the anticancer effects of DIM in SK-BR-3 cells using integrated cellular and molecular analyses. **Materials and Methods:** Cytotoxicity of DIM and its IC_{50} was determined by MTT (3-(4,5-dimethylthiazol-2-yl)-2,5-diphenyltetrazolium bromide) assay. The apoptotic efficacy of DIM was assessed using fluorescence microscopy with acridine orange/ethidium bromide (AO/EtBr) double staining, while intracellular reactive oxygen species (ROS) levels and mitochondrial membrane potential (MMP) were measured with a fluorescence-based assay and flow cytometry, respectively. Caspase-3 activity and Cell-cycle distribution were determined to evaluate activation of the apoptotic machinery and DNA content, respectively. NUMB and NOTCH2 expression levels were quantified, and molecular docking was performed to predict the interaction of DIM with NOTCH1. **Results:** DIM significantly reduced cell viability (IC_{50}: 154.27 µg/mL) and increased apoptotic cell populations compared with untreated cells ($p < 0.01$). Intracellular ROS levels increased, and the fluorescence intensity reached to ~9,000 arbitrary units in DIM-treated cells. DIM treatment increased mitochondrial depolarisation (8.25%) and Caspase-3 activity (0.85 units/mg protein) compared to untreated cells. DIM increased the G0/G1 and S-phase populations (70.7% and 20.1%, respectively), while the G2/M population was reduced (8.2%). DIM also increased NUMB expression and decreased NOTCH2 gene expression. DIM demonstrated a predicted affinity (binding energy: −5.3 kcal/mol) for the NOTCH1 receptor in the docking analysis. **Conclusion:** The findings of the present study suggest that DIM exhibits its anticancer activity in SK-BR-3 cells through multiple cellular pathways, with modulation of the NUMB/NOTCH axis. The predicted DIM–NOTCH1 interaction further supports a possible role of NOTCH signalling. Overall, the findings provide mechanistic insight into DIM activity and necessitate further investigation into its therapeutic potential.

Keywords: Caspase-3, DIM, Mitochondrial membrane potential, NOTCH2, NUMB, oxidative stress, ROS

Correspondence:
Rashed M. Almuqbil
Department of Pharmaceutical Sciences, College of Clinical Pharmacy, King Faisal University, Al-Ahsa 31982, SAUDI ARABIA.
Email: ralmuqbil@kfu.edu.sa

Received: 21-09-2026;
Revised: 18-10-2026;
Accepted: 26-10-2026.

www.ijper.org

INTRODUCTION

Breast cancer is the most prevalent disease diagnosed in women worldwide, and it has become a major health burden globally. Approximately 2.3 million new cases and 670,000 deaths were reported in 2022, with notable variations in incidence and mortality across socioeconomic and geographic contexts.[1,2] The heterogeneity of breast cancer is characterized by distinct factors resulting from the interplay of modifiable and non-modifiable factors, including genetic susceptibility, hormonal factors, metabolic alterations, lifestyle-related factors, chemical exposures, and epigenetic changes.[3] This suggests that the molecular mechanisms underlying its anticancer activity are still complex and appear to be influenced by the cellular environment.[4] Despite the efficacy of modern breast cancer therapies in saving lives, numerous instances of significant physical and psychological adverse effects have been documented. Moreover, the emergence of drug resistance threatens the efficacy of long-term treatments, prompting researchers to propose innovative therapeutic strategies.[5] Various studies demonstrated the anticancer efficacy of plant-based bioactive compounds through a number of mechanisms, including the induction of apoptosis and cell-cycle arrest, epithelial–mesenchymal

DOI: 10.5530/ijper.20270694

Copyright Information :
Copyright Author (s) 2027 Distributed under Creative Commons CC-BY 4.0

Publishing Partner : Manuscript Technomedia. [www.mstechnomedia.com]

transition, modification of inflammation and oxidative stress, and antiproliferation.[6]

The Chemopreventive and therapeutic potential of 3,3′-Diindolylmethane (DIM), a major bioactive metabolite of indole-3-carbinol (I3C), against cancer has been highlighted in recent reviews.[4] DIM is naturally derived from glucosinolates, found in cruciferous vegetables such as broccoli, cabbage, and cauliflower. DIM has been reported to inhibit cellular activities in breast cancer models by influencing the major intrinsic pathways involved in cancer cell proliferation and survival.[4] However, the molecular mechanisms underlying its anticancer activity remain complex and appear to depend on cellular context.[4,7] Therefore, evaluating ROS, mitochondrial membrane potential, and caspase activity can provide insight into its apoptotic effects. In addition, analysis of cell distribution across the G0/G1, S and G_2/M may provide further insight into its DIM-mediated antiproliferative mechanism.[8] NOTCH signalling is an important regulatory pathway involved in cellular differentiation, proliferation, and survival. NUMB acts as a negative regulator of NOTCH signalling, and loss of NUMB-mediated regulation may contribute to aberrant NOTCH activation and tumour progression.[9] Despite, the reported anticancer potential of DIM, its effects on the integrated relationship between cellular and biological contexts require further investigation. Therefore, this study investigated the anticancer activity of DIM in SK-BR-3 breast cancer cells using *in vitro* and *in silico* approaches, including cell viability, apoptosis, ROS, mitochondrial membrane potential, caspase-3, cell cycle, NUMB/NOTCH2 gene expression, and molecular docking with NOTCH1.

MATERIALS AND METHODS

Cell culture and compound preparation

The *in vitro* anticancer potential of DIM was evaluated in the SK-BR-3 (Human Breast Cancer) cell line (ATCC, USA). The cell line (Passage no 6) was cultured in Dulbecco's Modified Eagle's Medium (DMEM) (Sigma-Aldrich, USA), supplemented with FBS (10%), L-glutamine, sodium bicarbonate (Merck, Germany) and antibiotic solution. Cell lines were maintained at 37°C in a humidified 5% CO_2 incubator (NBS Eppendorf, Germany), and viability was tested frequently by inverted phase-contrast microscope and MTT assay. For *in vitro* analyses, 100 µL cell suspension ($5x10^3$ cells/well) from a two-day-old confluent monolayer was trypsinised and used. The stock solution of the compound was prepared by dissolving 1 mg of DIM in the same volume of 0.1% DMSO and filtered through a 0.22 µm Millipore syringe filter to ensure sterility before use in each experiment.

Estimation of Cell Viability

The viability of SK-BR-3 cells after DIM treatment was assessed using the MTT assay, following the method described by Mosmann.[10] Cells ($5x10^3$ cells/well) were treated with different concentrations of DIM, including 6.25, 12.5, 25, 50, and 100 µg/mL for 24 hr. The absorbance of the formazan product at 540 nm was measured using a microplate reader. The percentage of cell viability was calculated using the following formula: % viability = (Mean OD Samples x 100)/Mean OD of control group. IC_{50} value for DIM was calculated using ED50 PLUS V1.0 Software and used in subsequent assays.

Evaluation of Apoptotic Cell Death

Apoptotic activity of DIM in SK-BR-3 cells was evaluated using Acridine Orange/Ethidium Bromide (AO/EtBr) double staining, following the protocol of Zhang *et al.*[11] The cells ($5x10^3$ cells/well) were treated with DIM (IC_{50}) and incubated for 24 hr. After rinsing with cold Phosphate-Buffered Saline (PBS), the cells were stained with a mixture of AO (100 µg/mL) and EtBr (100 µg/mL) for 10 min at room temperature in the dark. Using fluorescence microscopy (Olympus CKX41 with Optika Pro5 camera) and nuclear morphology, the cells were categorised into viable, early apoptosis, and late apoptosis, and the percentage of cells in each category was calculated by counting at least 200 cells.

Determination of Intracellular Reactive Oxygen Species (ROS)

ROS levels were determined using 2′,7′-Dichlorofluorescein Diacetate (DCFDA) as described by Ramachandran and Saraswathy.[12] DIM-treated (IC_{50}) SK-BR-3 ($5x10^3$ cells/well) cells were incubated with DCFDA (50 µL) for 30 min. Fluorescence intensity was measured using a fluorescent microscope (Olympus CKX41 with optika pro5 CCD camera) at 485 nm excitation and emission at 535 nm (Qubit 3.0, Life technologies, USA) and expressed in Arbitrary Units (AU).

Determination of Mitochondrial Membrane Potential (MMP)

MMP was evaluated using the Muse™ MitoPotential Assay based on the instructions of the manufacturer. The working solution of The Muse™ MitoPotential Dye was prepared (1:1000) in 1× assay buffer. After trypsinisation, the DIM-treated (IC_{50}) SK-BR-3 cell ($5x10^3$ cells/well) suspension was mixed with 95 µL of mitopotential working solution and incubated at 37 °C for 20 min. Subsequently, Muse™ MitoPotential 7-AAD reagent (5 µL) was added and incubated for 5 min. MMP was then evaluated by flow cytometry (Millipore, USA), and events were acquired after gating and correlated with controls.

www.ijper.org

Determination of Caspase-3 Activity

SK-BR-3 cells were treated with DIM (154.27 µg/mL) for 24 hr. Following incubation, culture supernatants were collected, and 100 µL of each sample was added to a 96-well microplate and incubated overnight at 37 °C. The wells were washed twice with Phosphate-Buffered Saline (PBS) and blocked with 200 µL of 0.2% gelatin in PBS containing 0.05% Tween 20 for 1 hr at room temperature. After washing, 100 µL of primary anti-caspase-3 antibody (Santa Cruz Biotechnology; 1:500 dilution) was added and incubated for 2 hr at room temperature. Subsequently, the wells were washed and incubated with 100 µL of HRP-conjugated secondary antibody for 1 hr. Following washing, 200 µL of O-dianisidine hydrochloride substrate solution was added and incubated for 30 min. The reaction was stopped using 50 µL of 5 N HCl, and absorbance was measured at 415 nm.

Protein concentration was determined using the Bradford assay with bovine serum albumin as the standard. Relative caspase-3 immunoreactivity was expressed as the absorbance at 415 nm normalised to the measured protein concentration. Untreated SK-BR-3 cells served as the baseline control. No separate positive control for caspase-3 activation was included.[13]

Analysis of Cell Cycle Distribution

The cell suspension was centrifuged at 3000 rpm for 5 min to obtain a visible pellet, subsequently washed with an appropriate volume of PBS (1 mL of PBS per 1×10^6 cells). After centrifugation, the cell pellet was suspended in 50 µL of PBS (per 1×10^6 cells), subsequently fixed by the dropwise addition of ice-cold ethanol (70%) while vortexing at medium speed. After overnight freezing at −20 °C, the cell pellet was collected by centrifugation (as above) and washed with 250 µL of PBS. To the cell pellet, cell cycle reagent (250 µL) was added and incubated in the dark for 30 min. Flow cytometry analysis was performed to quantify the cell cycle distribution based on DNA content, and gating was performed with reference to untreated control cells.

Evaluating the interaction of DIM with NOTCH1 protein

Docking analysis was performed to evaluate the interaction of DIM with the NOTCH1 protein. The three-dimensional structure of DIM (PubChem CID: 3071) was obtained in Structure Data File (SDF) format, which was then converted to Protein Data Bank (PDB) format and subsequently prepared in PDBQT (PDB Partial Charge (Q), and Atom Type (T)) format for docking. The crystal structure of human NOTCH1 EGF-like repeats 11–13 (PDB ID: 2VJ3, Chain A) was used as the target protein. During receptor preparation, crystallographic water molecules and ionic heteroatoms were removed, and the cleaned receptor was converted to PDBQT format. Molecular docking was executed via AutoDock Vina.[14] The docking grid was positioned at coordinates −11.207, 6.648, and −21.545 Å, with dimensions of 20 × 20 × 20 Å and a grid spacing of 0.375 Å. Docking calculations were conducted with an exhaustiveness parameter of 8 and an energy range of 4 kcal/mol. The docking configurations were prioritised based on their predicted binding affinities, and the optimum binding mode was selected for interaction analysis.

Quantification of NUMB and NOTCH2 Gene Expression

Total RNA was isolated from DIM-treated SK-BR-3 and untreated cells (80% confluency) using TRIzol reagent (Invitrogen, USA). Briefly, cells were lysed with TRIzol reagent, followed by chloroform extraction and centrifugation. 100% isopropanol was added to the aqueous phase to precipitate the RNA, subsequently washed with ethanol (75%), air-dried, and resuspended in TE buffer. Complementary DNA (cDNA) was synthesized from 0.5 µg of total RNA using the iScript cDNA Synthesis Kit by setting the final volume to 20 µL and following the conditions: 25 °C (5 min), 46 °C (20 min), and 95 °C (1 min). Expression analysis of NOTCH2 and NUMB genes was performed using SYBR Green Master Mix on a LightCycler 96 real-time PCR system, set with conditions consisting of an initial activation step at 95 °C (2 min), followed by 40 cycles of denaturation at 95 °C (10 sec), annealing at 58 °C (1 min), and extension at 72 °C (1 min). GAPDH was used as the reference gene, and the relative gene expression was analyzed using the ΔΔCt method.

Statistical analysis

Results were expressed as mean ± SD. Statistical significance between control (untreated) and treated groups was determined using Student's *t*-test, and for varying compound concentrations, one-way ANOVA followed by Dunnett's multiple-comparison test was used. Differences were considered statistically significant at $^{**}p < 0.05$ and highly significant at $p < 0.01$.

RESULTS

Anticancer Activity of DIM

Untreated control cells showed ~100% viability, whereas treatment with DIM at varying concentrations ranging from 6.25 - 100 µg/mL gradually reduced cell viability to 97 - 67%, in a dose-dependent way (Figure 1G). Microscopic examinations (Figures 1A–F) revealed dose-dependent morphological changes and reduced cell density in the DIM-treated group (Figure 1A). The reduction in cell viability was statistically significant among the tested concentrations ($p < 0.05$ and $p < 0.01$, as shown in the Figure 1G). The calculated IC_{50} value for DIM was 154.27 µg/mL.

www.ijper.org

Apoptotic efficacy of DIM

The predominant green fluorescence observed in the untreated group indicated a significant proportion of live SK-BR-3 cells (Figure 2A). Conversely, DIM-treated (IC_{50} = 154.27 µg/mL) group showed increased orange/red fluorescence, indicating the incidence of apoptosis (Figure 2B). Quantitative assessment further confirmed a notable reduction in the proportion of viable cells from ~97% in the untreated group to ~42% in the DIM-treated group, as well as a significant (**$p < 0.01$) rise in both early (~20%) and late apoptotic cells (~35%) after DIM treatment (Figure 2C).

Effect of DIM on Intracellular ROS Levels

DIM treatment significantly increased green fluorescence relative to the untreated control group, indicating enhanced intracellular ROS generation (Figure 3A and B). Quantitative analysis further confirmed a significant ($p < 0.01$) increase in fluorescence intensity, from ~1,700 AU in the untreated group to ~9,000 AU in the DIM-treated group (Figure 3C), indicating increased intracellular ROS production that contributes to cytotoxicity and apoptosis in SK-BR-3 cells.

Mitochondrial Membrane Potential of DIM

Flow cytometric analysis showed that the percentage of depolarised live cells increased from ~3.85% in the control group (Figure 4A) to 8.25% with DIM treatment (Figure 4B). Quantitative analysis showed a notable rise in mitochondrial membrane depolarisation of 8.25 % in the group treated with DIM and 4% in the untreated group ($p < 0.01$) (Figure 4C), suggesting DIM-mediated mitochondrial dysfunction in SK-BR-3 cells.

Effect of DIM on Caspase-3 Activity

DIM-treated SK-BR-3 cells exhibited increased relative caspase-3 immunoreactivity compared with untreated control cells. The normalised absorbance values increased from 0.41 in the control group to 0.85 in the DIM-treated group, representing

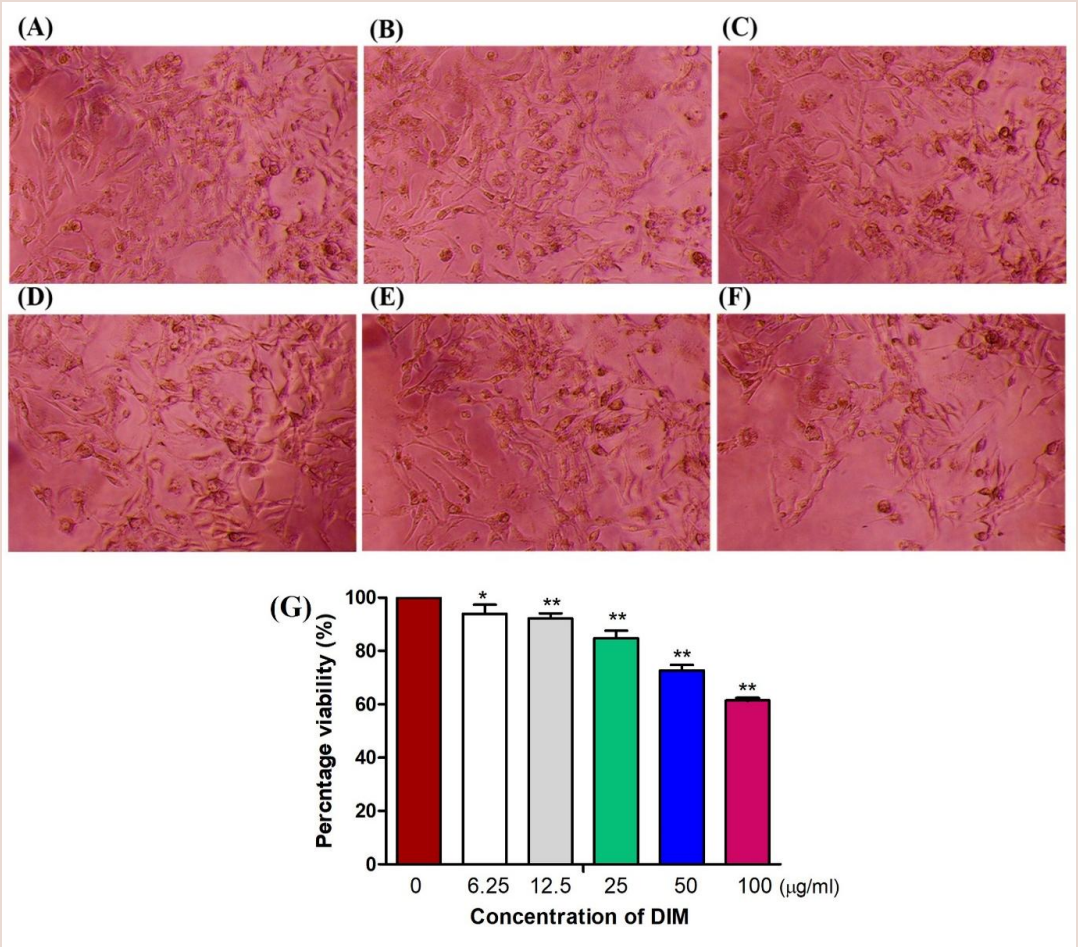

Figure 1: Effect of Diindolylmethane (DIM) on the viability of SK-BR-3 cells. Figure A-F: Representative phase-contrast microscopic images showing morphological changes in control (A) and treated groups: (B) 6.25, (C) 12.5, (D) 25, (E) 50 and (F) 100 µg/mL DIM for 24 hr. (G) Quantification of cell viability percentage determined by the MTT assay. Values represent mean ± SD (n = 3). Statistical significance was determined by one-way ANOVA followed by Dunnett's test; *$p < 0.05$ versus control.

www.ijper.org

an approximately 2.07-fold increase. These findings indicate increased caspase-3 antibody immunoreactivity following DIM treatment; however, the assay does not directly establish caspase-3 enzymatic activation (Figure 5).

Efficacy on Cell Cycle Distribution

The proportion of cells recorded in flow cytometry for the untreated group was 62.5, 8.8, and 28.3% in the G0/G1, S, and G_2/M phase, respectively. Meanwhile DIM-treatment increased the proportion of cells in the G0/G1 phase and S phase, with values of 70.7% and 20.1%, respectively, whereas the percentage in the G_2/M phase decreased markedly to 8.2% (Figure 6). The increase in the G0/G1 and S-phase populations was statistically significant ($p < 0.01$) (Figure 6C).

Molecular Docking of DIM with NOTCH1

Molecular docking analysis demonstrated that DIM exhibited a favorable predicted interaction with NOTCH1 (PDB ID: 2VJ3) with an affinity of −5.3 kcal/mol, which is the highest-ranked docking pose corresponding to Mode 1. The docked DIM molecule was located inside the close binding vicinity of NOTCH1, within 4.0 Å, and engaged with multiple neighboring amino acid residues. Seven residues were detected, specifically Phe474, Gln475, Cys476, Ile477, Cys478, Gly484, and Val485. A short-range polar contact was observed within the established 3.2 Å threshold, using the indole nitrogen of DIM. The two-dimensional interaction diagram (Figure 7A) depicts the primary contacting residues, such as Cys476, Gln475, Ile477, and Val485, while the three-dimensional model (Figure 7B) displays DIM situated on the NOTCH1 receptor's surface. The interaction profile indicates that DIM adopts a defined orientation within the receptor environment and establishes a polar contact through its indole nitrogen.

Effect of DIM on NUMB and NOTCH2 Gene Expression

After DIM treatment, NUMB expression increased to ~1.5-fold, whereas NOTCH2 expression decreased to ~0.7-fold compared with the untreated SK-BR-3 cells ($p < 0.01$) (Figure 8). The concurrent increase in NUMB and decrease in NOTCH2 suggests that DIM may modulate the NUMB/NOTCH signalling pathway, potentially contributing to its anticancer activity.

DISCUSSION

DIM has attracted considerable interest as a potential chemopreventive and anticancer agent because it can alter various intrinsic pathways contributing to cancer development.[15] Evidence suggests that DIM can modulate multiple cancer-associated processes, including cell proliferation, apoptosis, oxidative stress, mitochondrial function and cell-cycle progression.[4] The antiproliferative activity observed in the present study was

www.ijper.org

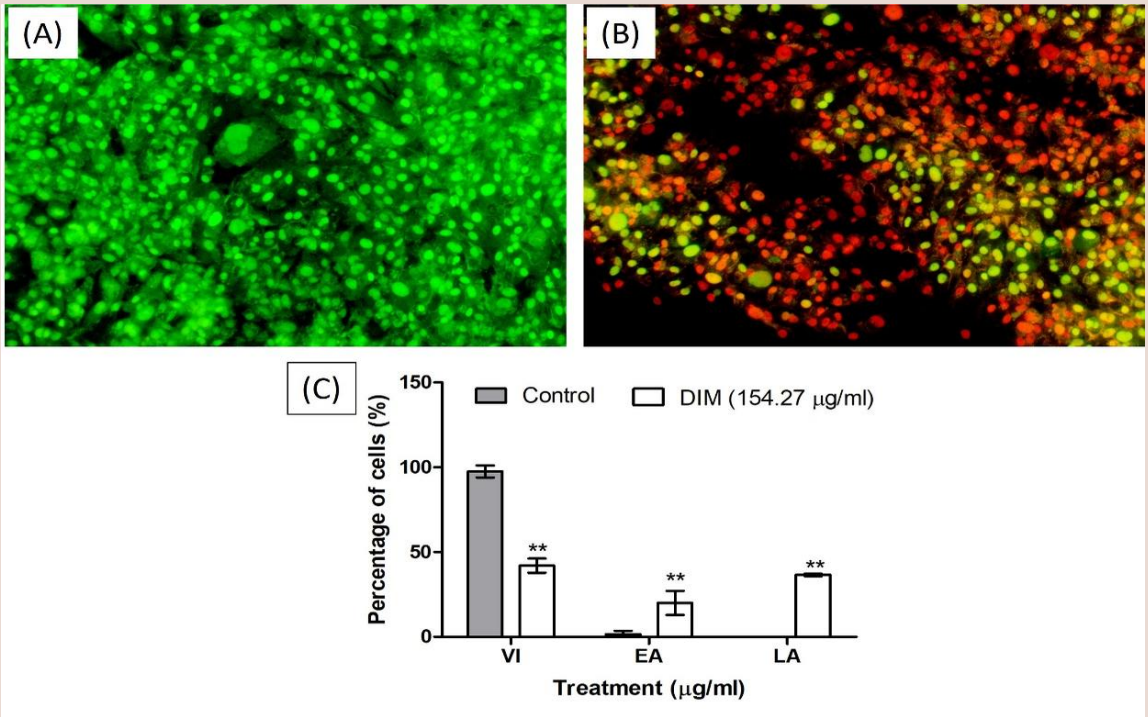

Figure 2: Determining Diindolylmethane (DIM)-induced apoptosis in SK-BR-3 cells by acridine orange/ethidium bromide double staining. (A) Untreated control cells showing predominantly green fluorescence. (B) Treated with DIM (154.27 µg/mL) for 24 hr, showing increased orange/red fluorescence. (C) Quantitative distribution of viable (VI), Early Apoptotic (EA), and Late Apoptotic (LA) cells in control and DIM-treated groups. Values are presented as mean ± SD (n=3); **$p < 0.01$ versus control.

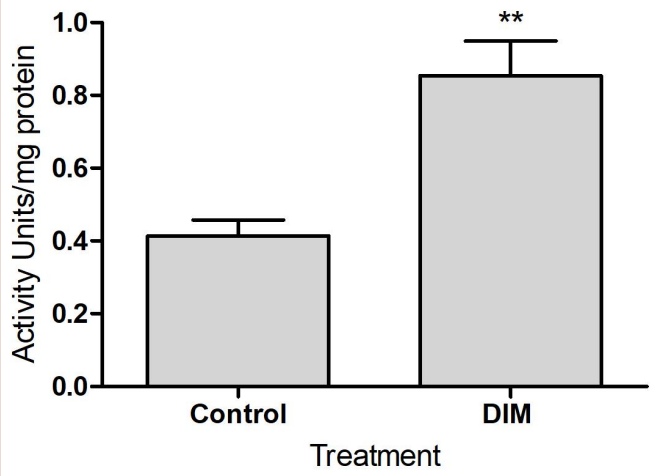

Figure 5: Graphical representation of ELISA results indicating the activation of caspase-3 in SK-BR-3 cells following Diindolylmethane (DIM) treatment (IC_{50}). Values are expressed as mean ± SD (n=3); **$p < 0.01$ versus control.

compared with a recent report evaluating DIM against MCF-7 breast cancer cells. In that study, DIM exhibited an IC_{50} of 202 µM (~ 49.7 µg/mL) after 24 hr of treatment.[16] Meanwhile, the present study showed an IC_{50} of 154.27 µg/mL (~626.5 µM), which may reflect differences in sensitivity due to experimental conditions and distinct biological characteristics of MCF-7 and SK-BR-3 cells. Lanza-Jacoby and Cheng reported that DIM at 25–50 µM showed a relatively modest reduction in SK-BR-3 cells compared with DIM (25 µM) and docetaxel (1 nM) combination, which reduced cell survival by ~59% after 48 hr.[17] In contrast, our study showed that DIM (100 µg/mL) alone was effective, reducing cell viability to ~61.5%, along with associated morphological changes and reduced cell density, supporting DIM's cytotoxic potential against SK-BR-3 cells.

The reduced cell viability accompanied by morphological alterations and an increase in the proportion of apoptotic cells indicated that the cytotoxic effect of DIM is at least partly mediated through programmed cell death. Lanza-Jacoby and Cheng.[17] reported that DIM enhanced apoptosis (~27.6%) in SK-BR-3 cells when DIM and docetaxel combination was used. Conversely, we observed that DIM alone markedly increased both the early and late apoptotic populations (~20% and 35%, respectively) ($p < 0.01$). Treatment with resveratrol (150 µM), a naturally occurring polyphenolic compound, resulted in ~7.27% early apoptotic and 23.48% late apoptotic cells, corresponding to a combined apoptotic population of ~30.75%.[18] The present study demonstrated a more pronounced apoptotic response following DIM (154.27 µg/mL) treatment, with cell viability decreasing

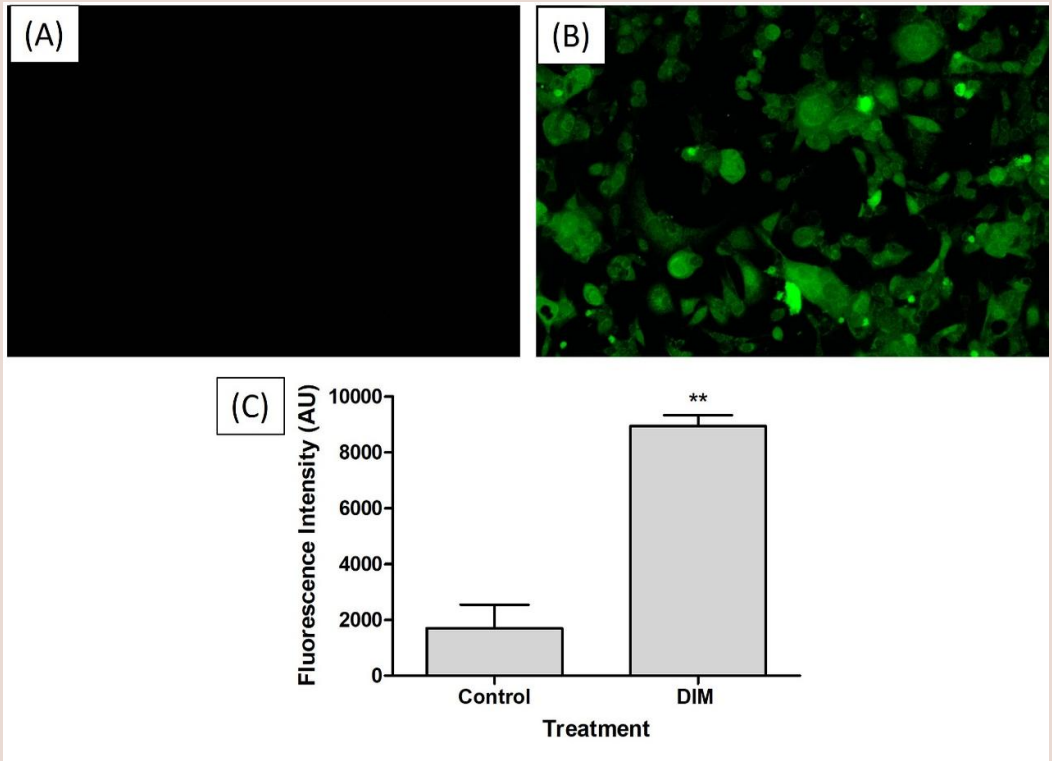

Figure 3: Diindolylmethane (DIM)-induced intracellular ROS generation in SK-BR-3 cells. Fluorescence images of (A) control and (B) DIM-treated cells (154.27 µg/mL) after 24 hr treatment and DCFDA staining. (C) Quantitative measurement of ROS-associated fluorescence intensity expressed in Arbitrary Units (AU). DIM treatment significantly increased intracellular fluorescence compared with the control. Values are presented as mean ± SD (n=3); **$p < 0.01$ versus control.

www.ijper.org

from ~97% in untreated cells to 42%, accompanied by an increase in the combined apoptotic population (~55%). The obtained values were significant and followed a pattern comparable to the apoptotic response reported for resveratrol in SK-BR-3 cells, although direct comparison of efficacy should be interpreted cautiously because of differences in compound concentration, treatment conditions, and experimental methodology.

ROS, a major regulator of cellular signalling, generally exhibit elevated levels due to altered metabolism and cancer signalling. Higher ROS accumulation can induce oxidative stress and selectively impair tumour-cell survival, suggesting an important mechanism for anticancer activity. According to recent evidence, plant-derived bioactive compounds can disrupt intracellular redox homeostasis and promote ROS accumulation.[19] In DCF-DA fluorescence analysis, tea tree oil (*Melaleuca alternifolia*), a plant-derived complex containing several terpenoid compounds, modestly increased the oxidative stress following 24 hr exposure. Fluorescence intensity increased from ~549 AU in untreated cells to 1,023 and 1,108 AU following treatment with 67.5 and 112.5 µg/mL tea tree oil, respectively.[20] Consistent with these observations, we observed a pronounced ROS elevation after 24 hr of DIM treatment and increased intracellular fluorescence intensity from ~1,700 AU in untreated cells to ~ 9,000 AU, indicating substantial ROS accumulation. The simultaneous increase in intracellular ROS and apoptotic cell populations further suggests that ROS accumulation may be associated with induction of apoptosis following DIM treatment.

Oxidative stress can damage mitochondrial components and subsequently disrupt membrane integrity and function, ultimately leading to mitochondrial membrane depolarisation.[21] Consistent with the above statement, we observed higher ROS levels and mitochondrial depolarisation in breast cancer cells after DIM treatment. DIM treatment significantly increased mitochondrial depolarisation from ~4% to 9% ($p < 0.01$) after 24 hr. Šebová *et al.* (2025) reported consistent results when they investigated the MMP potential of the metabolite Physodic Acid (PHY), found in

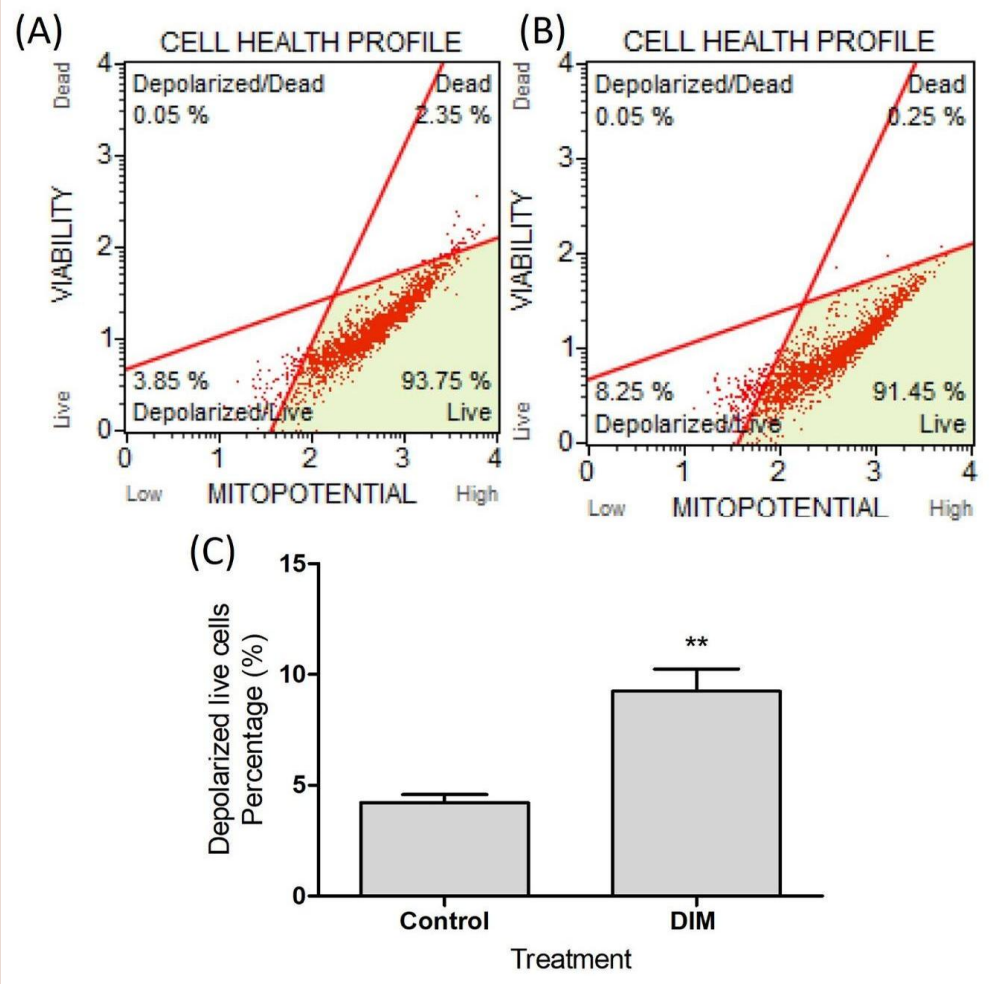

Figure 4: Efficacy of Diindolylmethane (DIM) on mitochondrial membrane depolarisation in SK-BR-3 cells. Flow cytometric profiles of (A) untreated control and (B) DIM-treated cells (IC_{50}) after 24 hr treatment. (C) Quantitative representation of live cells with depolarised mitochondria. Values are expressed as mean ± SD (n=3); **$p < 0.01$ versus control.

www.ijper.org

Pseudevernia furfuracea. PHY treatment increased the membrane depolarisation from 11.3% in the control group to 24.6% after 24 hr in SK-BR-3 cells, followed by a marked increase over time. Šebová *et al.* also documented mitochondrial dysfunction contributing to apoptosis, evidenced by phosphatidylserine externalisation, increased cell death, caspase activation, and PARP cleavage.[22] We observed a lower magnitude of DIM-induced depolarisation than with PHY, suggesting that the magnitude of mitochondrial depolarisation is highly contingent on the chemical structure of the compound and the precise exposure period. Therefore, DIM-mediated apoptosis may be triggered by mitochondrial dysfunction, which may interrupt the intrinsic pathway involved in programmed cell death.[23]

Persistent ROS can promote mitochondrial outer-membrane permeabilisation, which can then facilitate cytochrome c release; binding of which with the apoptotic protease-activating factor-1 (Apaf-1) forms a multiprotein complex. The protein complex is involved in the process of recruitment and activation of procaspase-9, subsequently activates caspases and promotes cell dismantling.[24] The significant increase in caspase-3 activity in SK-BR-3 cells supports the activation of the caspase-dependent apoptotic pathway following DIM treatment. In the present study, a ~2.1-fold increase in caspase-3 activity was recorded. Miao *et al.* reported that costunolide, a sesquiterpene lactone derived from *Aucklandia lappa*, induced apoptosis (SK-BR-3 cells) and exhibited an increase in caspase-3 expression by ~1.3, 1.6, and 2.1-fold with 10, 20, and 30 μM of costunolide, respectively, in 48 hr.[25] These findings suggest that DIM-mediated apoptosis may be triggered by the activation of the executioner caspase-3. Upon activation, caspase-3 cleaves a range of essential cellular substrates, including several inhibitor and cytoskeletal proteins, resulting in apoptosis by causing chromatin condensation, cell shrinkage, and other morphological alterations that lead to cell death.[26]

Altered checkpoint regulators mediate inappropriate cell cycle progression, a fundamental feature of cancer development, and can be suppressed by anticancer agents that induce accumulation at specific phases of the cell cycle.[27] DIM treatment significantly increased the proportion of cells in the G0/G1 phase (increased from 62.5 to 70.7%) and in the S phase (increased from 8.8 to 20.1%), whereas there was a marked reduction in the G2/M population (reduced from 28.3% to 8.2%). Miao *et al.*[25] demonstrated that costunolide (30 μM) treatment increased the percentage of SK-BR-3 cells in the G0/G1 phase, accompanied by a dose-dependent reduction in CDK2 and Cyclin E expression by 51.7% and 61.9%, respectively, indicating the disruption of the G1/S checkpoint. Although the cell-cycle response to DIM in this study differed from the G1 arrest caused by costunolide,

www.ijper.org

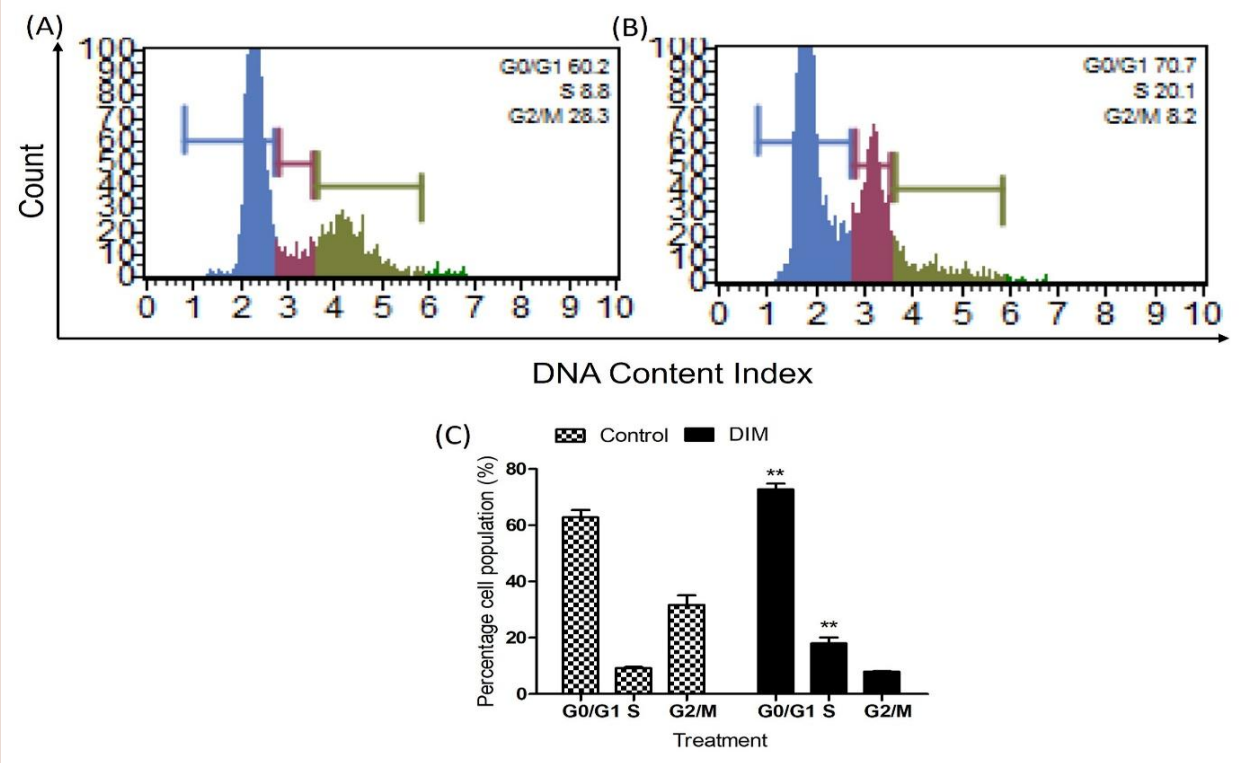

Figure 6: Efficacy of Diindolylmethane (DIM) in the alteration of cell cycle distribution in SK-BR-3 cells. Representative flow cytometric histograms showing DNA content and cell cycle distribution in (A) untreated control and (B) DIM-treated cells (IC_{50}, 24 hr). (C) Estimation of cells in the G0/G1, S, and G2/M phases. Values are expressed as mean ± SD (n=3); **p < 0.01 versus control.

DIM's impact on cell-cycle progression at the G1/S transition might disrupt the subsequent move toward G2/M. In another study, Chaga mushroom extract (0.5 mg/mL) increased the G0/G1 population from 56.5 to 76.1%; whereas the S-phase population decreased from 24.6 to 8.85% in 24 hr in SK-BR-3 cells. The authors attributed the accompanying disruption to cell-cycle regulatory proteins, including cycling and phosphorylated Rb.[28] These findings indicate that the influence of natural bioactive compounds on the cell cycle is mainly based on the molecular characteristics of the compound and the cellular processes.[29] DIM exposure may reflect interference with cell-cycle progression beyond the G1 checkpoint, as we observed the concomitant increase in S-phase cells and reduction in G2/M cells. Such alterations may also occur alongside oxidative stress, as ROS can modulate multiple cell-cycle regulatory processes and influence progression through the G1/S and G2/M transitions depending on their level and duration.[30]

To further explore the possible molecular basis of DIM's anticancer efficacy, we performed molecular docking analysis. The structural information on the possible binding orientation and interactions between a phytochemical and its protein target, obtained from the docking analysis, complements the above experimental findings with molecular-level insight. Molecular docking analysis demonstrated that the predicted binding affinity of DIM (−5.3 kcal/mol) falls within the range of binding energies reported for phytochemical–NOTCH complexes, supporting the plausibility of its interaction with NOTCH1. Shekar *et al.*[31] reported that Epigallocatechin Gallate (EGCG) exhibited a predicted binding affinity of −8.1 kcal/mol toward NOTCH1, and hydrogen-bond interactions involving Ala2006 and Arg1824 were found in the NOTCH1–EGCG complex. In Shekar *et al.* study, the docking energies reported across their phytochemical–protein complexes ranged from −9.4 to −5.1 kcal/mol. The predicted affinity may differ due to differences in ligand structure, interacting residues, binding orientation, and receptor structural models. In the present study, DIM interacted with several amino acid residues (Phe474, Gln475, Cys476, Ile477, Gly484, and Val485) in the 474–485 region of NOTCH1, along with a polar contact involving the indole nitrogen of DIM. These interactions indicate that DIM can adopt a stable orientation within the predicted NOTCH1 binding region. However, as molecular docking provides a computational prediction rather than experimental evidence of direct binding, further functional studies are required to confirm the DIM–NOTCH1 interaction. Resveratrol treatment reduced NOTCH1 expression and was associated with apoptotic and cell-cycle-related changes, providing experimental support for the involvement of NOTCH signalling in the anticancer activity of a phytochemical.[32]

The observed increase in NUMB expression together with the reduction in NOTCH2 expression following DIM treatment suggests that DIM may modulate the NUMB/Notch regulatory axis in SK-BR-3 cells. Sajadimajd *et al.*[33] reported the influence of PNA-antimiR-182 on NUMB-mediated NOTCH signalling in trastuzumab-sensitive as well as resistant SK-BR-3 cells. The increase in the intracellular level of the NOTCH inhibitor NUMB, accompanied by reduced levels of NICD and HES1, indicating attenuation of NOTCH1 signalling PNA-antimiR-182 treatment. Increased NUMB was also associated

www.ijper.org

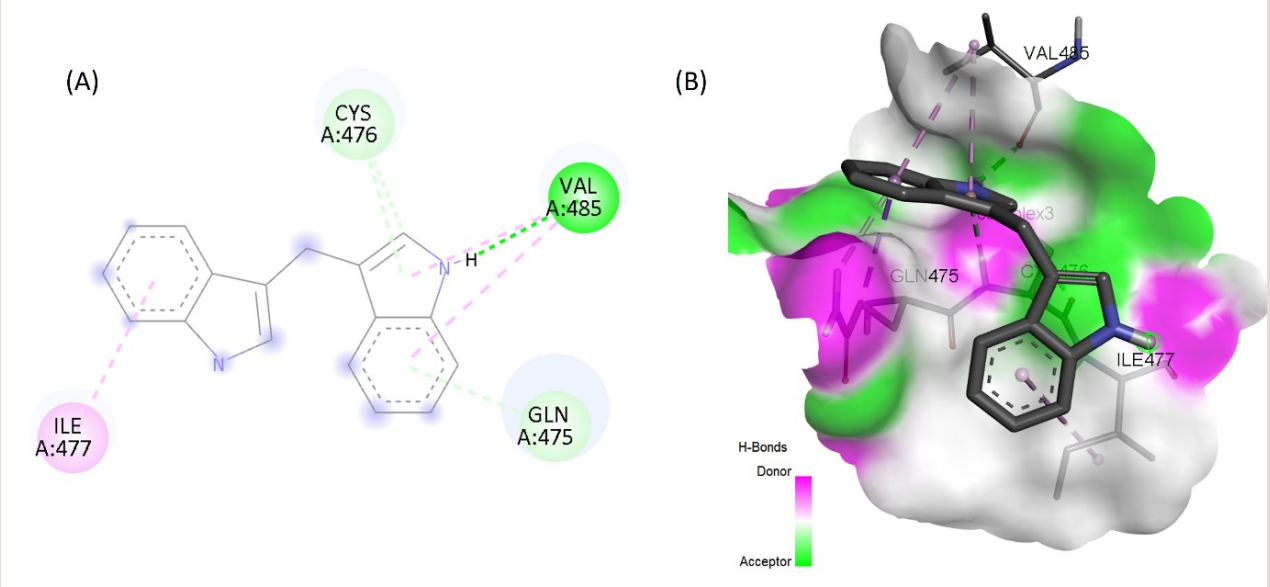

Figure 7: Molecular docking analysis of Diindolylmethane (DIM) with NOTCH1. (A) Two-dimensional representation of the predicted DIM–NOTCH1 interaction showing key contacting residues, including Phe474, Gln475, Cys476, Ile477, Cys478, Gly484, and Val485. (B) Three-dimensional surface representation showing the positioning of DIM within the NOTCH1 interaction environment.

with reduced HIF-1α expression and inhibition of proliferative and migratory properties in SK-BR-3 cells.[33] Increased Numb following Pin1 inhibition contributed to suppression of NOTCH1 signalling and the associated inhibition of proliferative and migratory properties of the resistant cells.[34] In the present study, DIM increased NUMB expression (~ 1.5-fold) while reducing NOTCH2 expression (~0.7-fold) relative to untreated cells. The findings suggest that DIM may attenuate NOTCH pathway activity and contribute to the antiproliferative and pro-apoptotic processes. Taken together, the findings suggest that DIM exhibits cytotoxicity and antiproliferative effects in SK-BR-3 cells through various mechanisms. DIM markedly increased intracellular ROS levels, suggesting oxidative stress that may contribute to MMP loss. Mitochondrial dysfunction was accompanied by increased apoptosis and approximately two-fold elevation of caspase-3 activity, supporting involvement of the caspase-dependent apoptotic machinery in DIM-induced cell death. In parallel, DIM altered cell-cycle distribution and modulated the NUMB/NOTCH signalling axis, which may contribute to the antiproliferative response. Therefore, further insight into the molecular mechanisms underlying DIM's anticancer activity is necessary to confirm the findings of the present study.

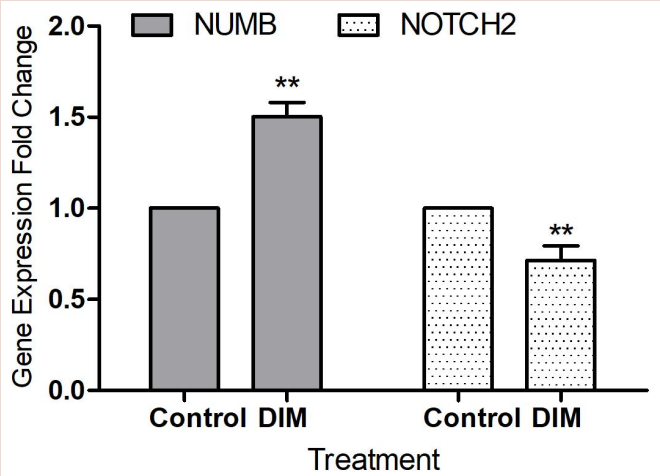

Figure 8: Results of PCR analysis showing modulation of NUMB and NOTCH2 gene expression following Diindolylmethane (DIM). Expression was normalised to GAPDH and analyzed using the $2^{-}\Delta\Delta Ct$ method. Values are expressed as mean ± SD (n=3); $^{**}p < 0.01$ versus untreated control.

CONCLUSION

In conclusion, DIM demonstrated *in vitro* cytotoxic and pro-apoptotic effects in SK-BR-3 breast cancer cells, accompanied by increased intracellular ROS levels, mitochondrial membrane depolarisation, and alterations in cell-cycle distribution. Modest but statistically significant changes in NUMB and NOTCH2 gene expression suggest a possible association with NOTCH-related signalling, while molecular docking provided an exploratory prediction of DIM interaction with NOTCH1. These preliminary findings support further investigation of DIM as a potential anticancer candidate. Additional studies involving protein-level validation, functional assays, and appropriate experimental models are required to establish the underlying mechanisms and therapeutic relevance.

ACKNOWLEDGEMENT

We are thankful to the Deanship of Scientific Research, Vice Presidency for Graduate Studies and Scientific Research, King Faisal University, Saudi Arabia, for their financial support.

ABBREVIATIONS

7-AAD: 7-Aminoactinomycin D; **AHR:** Aryl Hydrocarbon Receptor; **AO:** Acridine Orange; **ANOVA:** Analysis of Variance; **Apaf-1:** Apoptotic Protease-Activating Factor 1; **AU:** Arbitrary Units; **cDNA:** Complementary Deoxyribonucleic Acid; **CDK2:** Cyclin-Dependent Kinase 2; **DCFDA:** 2′,7′-Dichlorofluorescin Diacetate; **DIM:** 3,3′-Diindolylmethane; **DMEM:** Dulbecco's Modified Eagle Medium; **DMSO:** Dimethyl Sulfoxide; **DNA:** Deoxyribonucleic Acid; **EGCG:** Epigallocatechin Gallate; **ELISA:** Enzyme-Linked Immunosorbent Assay; **EtBr:** Ethidium Bromide; **FBS:** Fetal Bovine Serum; **GAPDH:** Glyceraldehyde-3-Phosphate Dehydrogenase; **GPX4:** Glutathione Peroxidase 4; **HES1:** Hairy and Enhancer of Split-1; **HIF-1α:** Hypoxia-Inducible Factor 1 Alpha; **HRP:** Horseradish Peroxidase; **I3C:** Indole-3-Carbinol; **IC_{50}:** Half-Maximal Inhibitory Concentration; **MMP:** Mitochondrial Membrane Potential; **MTT:** 3-(4,5-Dimethylthiazol-2-yl)-2,5-Diphenyltetrazolium Bromide; **NICD:** NOTCH Intracellular Domain; **NRF2:** Nuclear Factor Erythroid 2-Related Factor 2; **PBS:** Phosphate-Buffered Saline; **PDB:** Protein Data Bank; **PDBQT:** Protein Data Bank, Partial Charge (Q), and Atom Type (T) Format; **PHY:** Physodic Acid; **PI3K:** Phosphoinositide 3-Kinase; **ROS:** Reactive Oxygen Species; **RNA:** Ribonucleic Acid; **SD:** Standard Deviation; **SDF:** Structure Data File; **SK-BR-3:** Human Breast Cancer Cell Line SK-BR-3; **SYBR:** SYBR Green Fluorescent Dye; **TE:** Tris-EDTA; **ΔΔCt:** Comparative Threshold Cycle Method.

CONFLICT OF INTEREST

The authors declare that there is no conflict of interest.

www.ijper.org

FUNDING

This work was funded through the Deanship of Scientific Research, Vice Presidency for Graduate Studies and Scientific Research, King Faisal University, Al-Ahsa, Saudi Arabia [Grant Number KFU265283].

ETHICAL APPROVAL

There is no ethical approval needed for this research

SUMMARY

3,3′-Diindolylmethane (DIM) exhibited anticancer activity in SK-BR-3 breast cancer cells by reducing cell viability and promoting apoptosis. DIM increased intracellular reactive oxygen species, disrupted mitochondrial membrane potential, and enhanced caspase-3 activity. Treatment also altered cell-cycle distribution and modulated the NUMB/NOTCH signalling axis by increasing NUMB and decreasing NOTCH2 expression. Molecular docking predicted an interaction between DIM and NOTCH1. Collectively, these findings highlight multiple cellular and molecular mechanisms underlying DIM-mediated anticancer effects and warrant further investigation.

REFERENCES

1. Kim J, Harper A, McCormack V, *et al.* Global patterns and trends in breast cancer incidence and mortality across 185 countries. Nat Med. 2025;31(4):1154-62.
2. Ratheesh AP, Haridas S. Exploring the role of furan-pyrazole in the treatment of breast cancer: a comprehensive review. Asian J Pharm Health Sci. 2025;15(2):3073-82. doi:10.5530/ajphs.2025.15.79.
3. Anton SC, Lazan A, Grigore M, *et al.* Current trends in breast cancer genetics, risk factors, and screening strategies. J Biol Methods. 2025;12(2):e99010054.
4. Reyes-Hernández OD, Figueroa-González G, Quintas-Granados LI, *et al.* 3,3′-Diindolylmethane and indole-3-carbinol: potential therapeutic molecules for cancer chemoprevention and treatment via regulating cellular signaling pathways. Cancer Cell Int. 2023;23(1):180.
5. Masoodi G, Mir MA. Problems with currently used breast cancer treatments and side effects. In: Current Trends in Breast Cancer Pathology, Screening, Diagnosis and Treatments. Elsevier; 2026. p. 211-30.
6. Israel BeB, Tilghman SL, Parker-Lemieux K, Payton-Stewart F. Phytochemicals: current strategies for treating breast cancer. Oncol Lett. 2018;15(5):7471-8.
7. Guo L, Zhang J, Li Y, *et al.* 3,3′-Diindolylmethane induces ferroptosis and inhibits proliferation in non-small-cell lung cancer through the AHR/NRF2/GPX4 axis. Discov Oncol. 2025;16(1):344.
8. Rahman KW, Li Y, Wang Z, Sarkar SH, Sarkar FH. Gene expression profiling revealed survivin as a target of 3,3′-diindolylmethane-induced cell growth inhibition and apoptosis in breast cancer cells. Cancer Res. 2006;66(9):4952-60.
9. Pece S, Serresi M, Santolini E, *et al.* Loss of negative regulation by Numb over Notch is relevant to human breast carcinogenesis. J Cell Biol. 2004;167(2):215-21.
10. Mosmann T. Rapid colorimetric assay for cellular growth and survival: application to proliferation and cytotoxicity assays. J Immunol Methods. 1983;65(1-2):55-63.
11. Zhang JH, Yu J, Li WX, Cheng CP. Evaluation of Mn2+ stimulated and Zn2+ inhibited apoptosis in rat corpus luteal cells by flow cytometry and fluorochromes staining. Chin J Physiol. 1998;41(2):121-6.
12. Ramachandran R, Saraswathy M. Up-regulation of nuclear related factor 2 (NRF2) and antioxidant responsive elements by metformin protects hepatocytes against the acetaminophen toxicity. Toxicol Res. 2014;3(5):350-8.
13. Bradford MM. A rapid and sensitive method for the quantitation of microgram quantities of protein utilizing the principle of protein-dye binding. Anal Biochem. 1976;72(1-2):248-54.
14. Trott O, Olson AJ. AutoDock Vina: improving the speed and accuracy of docking with a new scoring function, efficient optimization, and multithreading. J Comput Chem. 2010;31(2):455-61.
15. Ho E, Wong CP, Bouranis JA, Shannon J, Zhang Z. Cruciferous vegetables, bioactive metabolites, and microbiome for breast cancer prevention. Annu Rev Nutr. 2025;45(1):171-95.
16. Singh S, Gupta N, Mishra DP, Verma S. Diindolylmethane containing peptides inhibit invasion and epithelial-mesenchymal transition associated gene expression in hormone-dependent breast cancer. Bioorg Med Chem. 2025:118421.
17. Lanza-Jacoby S, Cheng G. 3,3′-Diindolylmethane enhances apoptosis in docetaxel-treated breast cancer cells by generation of reactive oxygen species. Pharm Biol. 2018;56(1):407-14.
18. Li P, Liang Y, Ma X. Functional role of resveratrol in inducing apoptosis in breast cancer subtypes via inhibition of intracellular fatty acid synthase. Molecules. 2025;30(14):2891.
19. Escribano-Cebrián M, Bataller M, Biasini M, Garcia-Mayea Y, Virós D, LLeonart ME. Oxidative stress and cancer: current insights and therapeutic implications. Redox Biol. 2026:104355.
20. Seyhan MF, Dağdagül H, Eroğlu ÖN, Okumuş İ. Evaluation of the anti-carcinogenic effect of tea tree oil (*Melaleuca alternifolia*) on SK-BR-3 breast cancer cells. Int J Secondary Metab. 2026. Advance online publication.
21. Circu ML, Aw TY. Reactive oxygen species, cellular redox systems, and apoptosis. Free Radic Biol Med. 2010;48(6):749-62.
22. Sebova D, Zilakova S, Medvecova V, *et al.* Antiproliferative and pro-apoptotic effects of *Pseudevernia furfuracea* (L.) Zopf extract and its active component physodic acid via oxidative stress and DNA damage in breast cancer cells. Front Oncol. 2025;15:1557884.
23. Goldberg AA, Draz H, Montes-Grajales D, Olivero-Verbél J, Safe SH, Sanderson JT. 3,3′-Diindolylmethane (DIM) and its ring-substituted halogenated analogs (ring-DIMs) induce differential mechanisms of survival and death in androgen-dependent and androgen-independent prostate cancer cells. Genes Cancer. 2015;6(5-6):265.
24. Marcondes-de-Castro IA, Sales TA, Marinho TS, Aguila MB, Mandarim-de-Lacerda CA. Redox-sensitive coordination of mitochondrial quality control: integrating ROS, NAD+, and Ca2+ signaling in disease. Life Sci. 2026:124642.
25. Miao J, Chen J, Fan A, Luo J, Ma Q, Zhou N. Costunolide suppresses breast cancer progression in SK-BR-3 cells through CDK2/Cyclin E-mediated G1/S arrest, mitochondrial apoptosis, and PI3K/Akt-dependent inhibition of epithelial-mesenchymal transition. All Life. 2026;19(1):2637253.
26. Unnisa A, Greig NH, Kamal MA. Inhibition of caspase 3 and caspase 9 mediated apoptosis: a multimodal therapeutic target in traumatic brain injury. Curr Neuropharmacol. 2023;21(4):1001-12.
27. Moloudi K, Abrahamse H, George BP. Photodynamic therapy induced cell cycle arrest and cancer cell synchronization. Front Oncol. 2023;13:1225694.
28. Wang J, Beghelli D, Amici A, *et al.* Chaga mushroom triterpenoids inhibit dihydrofolate reductase and act synergistically with conventional therapies in breast cancer. Biomolecules. 2024;14(11):1454.
29. Bailon-Moscoso N, Cevallos-Solorzano G, Carlos Romero-Benavides J, Isabel Ramirez Orellana M. Natural compounds as modulators of cell cycle arrest: application for anticancer chemotherapies. Curr Genomics. 2017;18(2):106-31.
30. Sauer H, Wartenberg M, Hescheler J. Reactive oxygen species as intracellular messengers during cell growth and differentiation. Cell Physiol Biochem. 2001;11(4):173-86.
31. Shekar N, Vuong P, Kaur P. Analysing potent biomarkers along phytochemicals for breast cancer therapy: an *in silico* approach. Breast Cancer Res Treat. 2024;203(1):29-47.
32. Pandey P, Ramniwas S, Seifeldin SA, *et al.* Notch signaling mediated repressive effects of resveratrol in inducing caspase-dependent apoptosis in MCF-7 breast cancer cells. Cell Mol Biol (Noisy-le-grand). 2024;70(8):96-103.
33. Sajadimajd S, Yazdanparast R, Akram S. Involvement of Numb-mediated HIF-1α inhibition in anti-proliferative effect of PNA-antimiR-182 in trastuzumab-sensitive and-resistant SKBR3 cells. Tumour Biol. 2016;37(4):5413-26.
34. Sajadimajd S, Yazdanparast R. Sensitizing effect of juglone is mediated by down regulation of Notch1 signaling pathway in trastuzumab-resistant SKBR3 cells. Apoptosis. 2017;22(1):135-44.

Cite this article: Almuqbil RM. Diindolylmethane-Mediated Apoptosis and Cell Cycle Alterations in SK-BR-3 Breast Cancer Cells: Cellular, Molecular and In Silico Approaches. Indian J of Pharmaceutical Education and Research. 2027;1-11.

www.ijper.org